Photoisomerization Behavior of Bisbenzylidene and 1,3,4-Oxadiazole-Based Liquid Crystalline Polyesters

R. Balamurugan, P. Kannan

Department of Chemistry, Anna University, Chennai 600 025, Tamil Nadu, India

Received 30 June 2009; accepted 9 November 2009
DOI 10.1002/app.31742
Published online 5 January 2010 in Wiley InterScience (www.interscience.wiley.com).

ABSTRACT: Photoisomerization behavior of bisbenzylideneacetone/cycloheptanone and 1,3,4-oxadiazole containing nematic liquid crystalline polyesters under UV irradiation was investigated. Solubility, carbonyl group absorption band in FTIR, optical microscopy observation, as well as DSC analysis through existence of liquid crystallinity after irradiation were proved this phenomenon. Fluorescence spectra revealed blue-emission maxima with Stokes shift in the range of 46–49 nm. Band gap energy calculated from absorption spectra are in the range of 3.18–3.41 eV. Structure–property relationships were probed by correlating the spacer length with development of mesophase formation, thermal, and optical properties. Optical property of polymers disclosed photoisomerization processes. © 2010 Wiley Periodicals, Inc. J Appl Polym Sci 116: 1902–1912, 2010

Key words: liquid crystalline polymer; bisbenzylidene chromophore; 1,3,4-oxadiazole; photoisomerization; optical property; fluorescence

INTRODUCTION

Chalcones are widely employed as mesogen in liquid crystalline polymers and well-known photoactive chromophores. The chalcones such as cinnamates, benzylidenephthalimidines, benzylideneacetophenones, stilbazoles, coumarins, and diphenylacetylenes were employed for photo alignment and photocrosslinking segment in polymers.[1,2] Extensive studies have been made on photo alignment induced by thin film of polymers with photodimerizable side chains.[3–5]

The mesogenic moiety plays an important role in determining physical property of main chain liquid crystalline polymers (MCLCPs). The characteristic LC behavior possesses an essential relationship with molecular interaction between mesogens and structural elucidation in molecular level assumed to be a significant relevance in MCLCPs.[6] The various fluorescent species in polymers, such as monomeric chromophore, excimer, and ground-state complex, were demonstrated in molecular interaction within the segment of polymers.[7–10]

Exploring the conjugated 1,3,4-oxadiazole (OD) containing simple compound and polymer contributed to host new materials favorable for opto-electronics not only improved balance of charge mobility but also enhanced thermal and photo stability as well. The robust functionality and many documented synthetic routes, 1,3,4-oxadiazole has been recently incorporated into small molecular mixture,[11,12] side-chain,[13,14] and polymer[15,16] to increase external quantum efficiency with overall device performance.[17–19] On the other hand, the polymers containing heterocyclic moieties such as oxadiazole, thiazole, triazole, etc. are proved as fluorescent as well as highly thermally stable materials in various applications. The drawback of 1,3,4-oxadiazole-based polymer is its poor solubility and lack of in-depth understanding to specific contribution in optical and electronic characteristics. The issue of solubility has been handled by incorporation of flexible side-chains, often alkoxy structure of varying lengths to rigid oxadiazole moiety over come this draw back.[20,21]

There was a report on photoisomerization of bisbenzylideneacetophenone in a compound[22] but no report available on photoisomerization for a compound and or a polymer film containing bisbenzylideneacetone (BBA)/bisbenzylidenecycloheptanone moieties (BBCHep). The salient feature of this work is the synthesis and characterization of bisbenzylideneacetone/cycloheptanone and 1,3,4-oxadiazole-based polymers and established their photoisomerization behavior. Herein, we are reporting hitherto unreported photolysis observed under UV light and effect of methylene spacer on structure–property relationship particularly, thermal, mesomorphic, and optical properties of semirigid thermotropic main chain liquid crystalline polyesters containing photochromic bisbenzylideneacetone/cycloheptanone and

Additional Supporting Information may be found in the online version of this article.

Correspondence to: P. Kannan (pakannan@annauniv.edu).

1,3,4-oxadiazole segments which are expected to form thin film and finds wide applications in photo curable coatings, photolithography, optical data storage and information display, fabricating anisotropic networks, LC elastomers and thermosets, etc.

EXPERIMENTAL

Materials

Cycloheptanone (Aldrich), acetone (Merck), and thionyl chloride (Spectrochem, India) were used as received. Solvents were purified and dried by reported procedures before use.[23,24] 6-Bromo-1-hexanol,[25] 8-bromo-1-octanol,[26] and 10-bromo-1-decanol,[27] and precursors namely 2,7-bis[4-hydroxybenzylidene] cycloheptanone (BHBCHep), 2,2′-bis(4-hydroxybenzylidene)acetone (BHBA),[28] 2,5-bis(4-methylphenyl)-1,3,4-oxadiazole(BMPOD),[29] 2,5-bis(4-carboxylphenyl)-1,3,4-oxadiazole (BCPOD),[30] and monomer namely, 2,5-bis(4-phenylacyl chloride)-1,3,4-oxadiazole (BPACOD)[31] were prepared by the procedures reported elsewhere.

Instrumentation

The intrinsic viscosity of polymers was determined in an Ubbelohde viscometer using chloroform as a solvent at 30°C. Infrared spectra were obtained on a Thermomattson satellite model FTIR spectrometer using KBr pellet. High-resolution ^{1}H- and ^{13}C-NMR spectra were recorded on a Bruker spectrometer at 500 MHz using $CDCl_3$. Tetramethylsilane (TMS) was used as an internal standard. TGA thermograms were recorded on a NETZSCH-Gerâtebau Gmbh thermal analysis system. The DSC measurements were performed on a Mettler Toledo STAR^{e} system at a heating rate of 10°C/min up to 500°C on sample taken in an aluminum pan with a pierced lid, in dry nitrogen atmosphere with an empty pan as reference. For some samples cooling also applied with the rate of 10°C/min. The melting temperatures (T_m) and the liquid crystalline to isotropic phase transition temperatures (T_i) were taken as maximum of endothermic peaks. Hot stage optical polarized microscopy (HOPM) studies were performed on a Euromex polarizing microscope equipped with a Linkem HFS 91 heating stage and a TP-93 temperature programmer. Small quantity of sample was placed between two thin glass cover slips, heating and cooling done at a rate of 5°C min^{-1} and observed the mesophase. Elemental analysis was performed using Perkin Elmer 2400 elemental analyzer. Photoisomerization behavior was investigated by observing absorptions between 320 and 420 nm on a Shimadzu UV-160A UV–Visible recording spectrophotometer in both thin film and chloroform solution (10^{-2M}). Typical procedure adopted is as follows: Polymer film was formed on quartz plate and subjected to UV irradiation emanating from a 125 W medium pressure mercury lamp kept at a distance of 10 cm from sample at various intervals of time followed by UV absorption measured on the spectrophotometer, respectively. This procedure was repeated until reduction in absorption completed. Fluorescence spectra of polymers were obtained on a Shimadzu RF-5301PC spectrofluorimeter with excitation near absorption maxima of oxadiazole moiety with resolution of 5 nm for both excitation and emission.

Synthesis of benzylidene monomers

2,2′-Bis[4-(*m*-hydroxyalkyloxy)benzylidene)]acetone (m = 6,8,10) (ia–ic)

Synthesis of monomer ia. 2, 2′-bis(4-hydroxybenzylidene)acetone (BHBA) (10 mmol) was dissolved in dry dimethylformamide (20 mL), then potassium carbonate (50 mmol) added to it. Instantly, yellow color solution changed to red was noticed as an indication of formation of anions. The temperature of the reaction mixture was kept at 90°C for 1 h. Subsequently, 6-bromo-1-hexanol (25 mmol) was added dropwise to the mixture and then stirring continued at 90°C for 24 h. At the end of reaction, the mixture was cooled and poured over crushed ice to precipitate the product. Then, it was filtered, washed with excess of distilled water followed by *n*-hexane, recrystallized from ethanol–water mixture (50 : 50), and dried in vacuo at 50°C for 6 h (yield 79%; m.p.140–142°C).[32]

IR (KBr): 1684 cm^{-1} ($\nu_{C=O}$), 3376 cm^{-1} (spacer OH) and 1569 cm^{-1} ($\nu_{C=C}$ exocyclic); ^{1}H-NMR-δ: 9.0(s, 2H, O*H*), 7.5(s, 2H, C*H*=), 6.9–7.3(m, 6H, Aromatic-*H*), 3.0(s, 4H, βCH_2), 1.6(s, 2H, γCH_2), 2.1–2.5(m, 16H, CH_2 spacer), 3.8(t, 8H, —OCH_2). ^{13}C-NMR ($CDCl_3$) δ: 25–28(Ar—O—CH_2—CH_2—), 64–67 (Ar—O—CH_2—), 126–129(aromatic carbons). Elem. Anal. Calcd. for $C_{29}H_{38}O_5$ (466.2): C, 74.63; H, 8.26. Found: C, 74.42; H, 8.12.

The remaining monomers namely, 2,2′-bis[4-(8-hydroxyoctyloxy) benzylidene]acetone (**ib**) and 2,2′-bis[4-(10-hydroxydecyloxy)benzylidene]acetone (**ic**) were prepared by adopting the similar procedure wherein, 8-bromo-1-octanol and 10-bromo-1-decanol were used, respectively, instead of 6-bromo-1-hexanol.

2,2′-Bis[4-(8-hydroxyoctyloxy) benzylidene]acetone (ib). Yield 78%; m.p.135–137°C.IR (KBr): 1679 cm^{-1}($\nu_{C=O}$), 3396 cm^{-1}(spacer OH) and 1590 cm^{-1} (νC=C exocyclic). ^{1}H-NMR-δ: 8.5(s, 2H, O*H*), 7.8 (s, 2H, C*H*=), 7.0–7.4(m, 6H, Aromatic-*H*), 2.6(s, 4H, βCH_2),1.9(s, 2H, γCH_2), 2.4–2.7(m, 24H, CH_2 spacer), 3.9(t, 4H,

—OCH_2). ^{13}C-NMR ($CDCl_3$)δ: 26–29(Ar—O—CH_2—CH_2—), 69 (Ar—O—CH_2—), 130–137 (aromatic carbons). Elem. Anal. Calcd. for $C_{33}H_{46}O_5$ (522.26): C, 75.71; H, 8.68. Found: C, 75.79; H, 8.93.

2,2′-Bis[4-(10-hydroxydecyloxy)benzylidene]acetone (ic). Yield 82%; m.p.131–133°C.IR (KBr): 1683 cm^{-1} ($\nu_{C=O}$), 3395 cm^{-1} (spacer OH) and 1592 cm^{-1} ($\nu_{C=C}$ exocyclic) ^{1}H-NMR-δ: 9.0(s, 2H, O*H*), 7.4 (s, 2H, C*H*=), 6.8–7.4(m, 6H, Aromatic-*H*), 3.0(s, 4H, βCH_2), 1.8(s, 2H, γCH_2), 1.8–2.5(m, 32H, CH_2spacer), 3.6 (t, 8H, —OCH_2). ^{13}C-NMR ($CDCl_3$)δ: 26–30(Ar—O—CH_2—CH_2—), 68 (Ar—O—CH_2—), 129 (aromatic carbons). Elem. Anal. Calcd. $C_{37}H_{54}O_5$ (578.76): C, 76.71; H, 9.38. Found: C, 76.83; H, 9.48.

2,7-Bis[4-(*m*-hydroxyalkyloxy)benzylidene]cycloheptanone (*m* = 6, 8, 10)(iia–iic)

A similar procedure followed for the synthesis of monomer **ia** was adopted for the preparation of 2, 7-bis [4-(m-hydroxyalkyloxy)benzylidene]cycloheptanone monomers.

2,7-Bis[4-(6-hydroxyhexyloxybenzylidene)]cycloheptanone (BHHBCHp) (iia). (Yield 84 %; m.p. 144–146°C). IR (KBr): 1674 cm^{-1}($\nu_{C=O}$), 1581 cm^{-1}($\nu_{C=C}$ exocyclic). ^{1}H-NMR ($CDCl_3$, TMS): 7.4(s, 2H, O*H*), 6.8–7.2(m, 6H, Aromatic-*H*), 6.2(s, 2H,—C*H*=CH—), 3.4(t, 8H, OCH_2 spacer), 2.7(s, 4H, βCH_2), 1.7(s, 2H, γCH_2), 1.9–2.4(m, 16H, CH_2 spacer). ^{13}C-NMR ($CDCl_3$) δ: 25–29(Ar—O—CH_2—CH_2—), 64 (Ar—O—CH_2—), 129(aromatic carbons). Elem. Anal. Calcd. for $C_{33}H_{44}O_5$ (520.46): C, 76.14; H, 8.50. Found: C, 76.19; H, 8.63.

2,7-Bis[4-(8-hydroxyoctyloxybenzylidene)]cycloheptanone (BHOBCHp) (iib). Yield 83%; m.p.141–143°C. IR (KBr): 1670 cm^{-1} ($\nu_{C=O}$), 1582 cm^{-1} ($\nu_{C=C}$ exocyclic). ^{1}H-NMR ($CDCl_3$)-δ: 8.1(s, 2H, O*H*), 6.8–7.4(m, 6H, Aromatic-*H*), 3.5(t, 8H, OCH_2 spacer), 2.9 (s, 4H, βCH_2). 1.6 (s, 2H, γCH_2), 1.7–2.4(m, 24H, CH_2). ^{13}C-NMR ($CDCl_3$) δ: 26–29(Ar—O—CH_2—CH_2—), 65 (Ar—O—CH_2—), 127(Aromatic carbon). Elem. Anal. Calcd. for $C_{37}H_{52}O_5$ (576.76): C, 77.06; H, 9.12. Found: C, 77.19; H, 9.17.

2,7-Bis[4-(10-hydroxydecyloxybenzylidene)]cycloheptanone (BHDBCHp) (iic). Yield 80%; m.p.137–138°C. IR (KBr): 1672 cm^{-1}($\nu_{C=O}$), 1579 cm^{-1} ($\nu_{C=C}$ exocyclic). ^{1}H-NMR-δ: 6.9–7.3(m, 6H, Aromatic-*H*), 7.8(s, 2H, O*H*), 4.0(s, 3H, OCH_3), 3.2(t, 8H, OCH_2 spacer), 2.9(s, 4H, CH_2). 1.7(s, 2H, γCH_2), 1.8–2.5(m, 32H, CH_2). ^{13}C-NMR ($CDCl_3$) δ: 27–29(Ar—O—CH_2—CH_2—), 66 (Ar—O—CH_2—), 129 (aromatic carbon). Elem. Anal. Calcd. $C_{41}H_{60}O_5$ (632.46): C, 77.78; H, 9.55. Found: C, 77.89; H, 9.71.

Synthesis of polymers

Photoreactive LC polyesters were prepared by solution polycondensation technique at ambient temperature using triethyl amine (TEA) as an acid acceptor. A typical procedure for the synthesis of polymer **Ia** (poly{2,2′-bis[4-(6-hexyloxy)benzylideneacetone-2,5-bis(4-phenyl)-1,3,4-oxadiazole dicarboxylate]}) is as follows: The monomer **ia** (10 mmol) was dissolved in dry THF (20 mL), TEA (20 mmol) added and stirred for 5 min. BPACOD (10 mmol) was dissolved in THF (20 mL) added dropwise to the reaction mixture at ambient temperature and reaction continued for 24 h. At the end of reaction, the mixture was concentrated, cooled, and poured into excess of methanol. A yellow colored precipitate thus formed was purified by reprecipitation using THF-methanol, filtered, and dried in a vacuum oven at 50°C (Yield 81%). The other polymers namely, poly{2,2′-bis[4-(8-octyloxy)benzylideneacetone-2,5-bis(4-phenyl)-1,3,4-oxadiazole dicarboxylate]} (**Ib**) and poly{2,2′-bis[4-(10-decyloxy)benzylideneacetone-2,5-bis(4-phenyl)-1,3,4-oxadiazole dicarboxylate]}(**Ic**) were prepared in an analogous manner and representative spectral values of polymer **Ia** is given as follows.

IR (KBr, cm^{-1}): 1070 ($\nu_{C—O—C}$ in oxadiazole ring), 1472 (—N=N—), 1718 (ester carbonyl), 1602(exocyclic—C=C— of benzylidene), 723 (aromatic ring), 832 (—CH of aromatic ring), 1415 (presence of para-substitutions). ^{1}H-NMR ($CDCl_3$, δ): 6.8–7.6 (m, aromatic protons), 1.3–1.7 (s, —CH_2 protons in the spacer), 3.9 (d, Ar—O—CH_2), 7.8 (s, olefinic proton). ^{13}C-NMR ($CDCl_3$, δ): 68.0 (Ar—O—*C*), 169.2 (*Ar*—O—C), 28–29 (Ar—O—C—*C*), 167.48 (—*C*=O— group of ester carbonyl), 186.35 (—C=O— group in alkanone). Elemental analysis data were tabulated in Table I.

Poly{2,7-bis[4-(*m*-alkyloxy)benzylidenecycloheptanone-2,5-bis(4-phenyl)-1,3,4-oxadiazole dicarboxylate]}s (IIa–IIc)

A similar procedure adopted for the synthesis of polymer **Ia** was followed in the preparation of poly{2,7-bis[4-(6-hexyloxy) benzylidenecycloheptanone-2,5-bis(4-phenyl)-1,3,4-oxadiazole dicarboxylate]}s (**IIa**). The other polymers **IIb** and **IIc** were prepared in an analogous manner and the representative spectral values of polymer **IIa** is given as follows.

IR (KBr, cm^{-1}): 1007 ($\nu_{C—O—C}$ in oxadiazole ring), 1468 (—N=N—), 1725 (ester carbonyl), 1598 (exocyclic—C=C— of benzylidene), 775 (aromatic ring), 860 (—CH of aromatic ring), 1411 (presence of para-substitutions). ^{1}H-NMR ($CDCl_3$, δ): 6.77–7.98 (m, aromatic protons), 1.24–1.74 (s, -CH_2 protons in the spacer), 4.12 (d, Ar—O—CH_2), 7.31 (s, olefinic proton). ^{13}C-NMR ($CDCl_3$, δ): 65.47 (Ar—O—C), 157.9.2 (*Ar*—O—C), 28–29 (Ar—O—C—*C*), 165.94 (—*C*=O— group of ester carbonyl), 188.17 (—C=O— group in alkanone).

TABLE I
Yield, Viscosity, Solubility and Elemental Analysis Data of Polymers Ia–Ic and IIa–IIc

Polymer	Yield %	η_{int}[a] (dl/g)	Solubility[b] DMF	$CHCl_3$	DCM	THF	MeOH	EtOH	Benzene	Emp.formula (Form.wt)	Elemental analysis	C	H	N
Ia	89	0.54	+/+	+/+	+/+	+/+	−/−	−/−	−/−	$(C_{39}H_{32}N_2O_8)_n$ (656.61)$_n$	Calc.	71.13	5.22	4.24
											Found	71.18	5.09	4.08
Ib	79	0.60	+/+	+/+	+/+	+/+	−/−	−/−	−/−	$(C_{41}H_{36}N_2O_8)_n$ (684.69)$_n$	Calc.	71.68	5.54	4.11
											Found	71.96	5.33	3.97
Ic	86	0.65	+/+	+/+	+/+	+/+	−/−	−/−	−/−	$(C_{43}H_{40}N_2O_8)_n$ (712.59)$_n$	Calc.	72.17	6.03	4.04
											Found	72.69	5.94	3.84
IIa	88	0.78	+/+	+/+	+/+	−/+	−/−	−/−	−/−	$(C_{43}H_{38}N_2O_8)_n$ (710.32)$_n$	Calc.	72.41	5.57	4.06
											Found	72.34	5.87	3.91
IIb	76	0.91	+/+	+/+	+/+	−/+	−/−	−/−	−/−	$(C_{45}H_{42}N_2O_8)_n$ (738.32)$_n$	Calc.	72.59	5.68	3.89
											Found	72.76	5.84	3.96
IIc	81	1.02	+/+	+/+	+/+	+/+	−/−	−/−	−/−	$(C_{47}H_{46}N_2O_8)_n$ (766.69)$_n$	Calc.	73.57	6.21	3.71
											Found	73.99	6.36	3.83

[a] Measured at 30°C with $c = 0.2$ g/dl in chloroform.
[b] Solubility of polymers (0.05 g in 10 mL); +/+, soluble at room temperature; −/+, soluble on heating; −/−, insoluble.

RESULTS AND DISCUSSION

Synthesis and characterization

The strategy adopted in the polymer synthesis is shown in Scheme 1. Chain extended chalcones were synthesized under Williamson aryl-alkyl ether synthesis and dehydrocyclization employed by polyphosphoric acid for the synthesis of 1,3,4-oxadiazole. 2, 5-Bis(4-phenylacyl chloride)-1,3,4-oxadiazole and chain extended diols of chalcone units such as bisbenzylidenecycloheptanone/acetone with varying spacer lengths were polymerized by solution

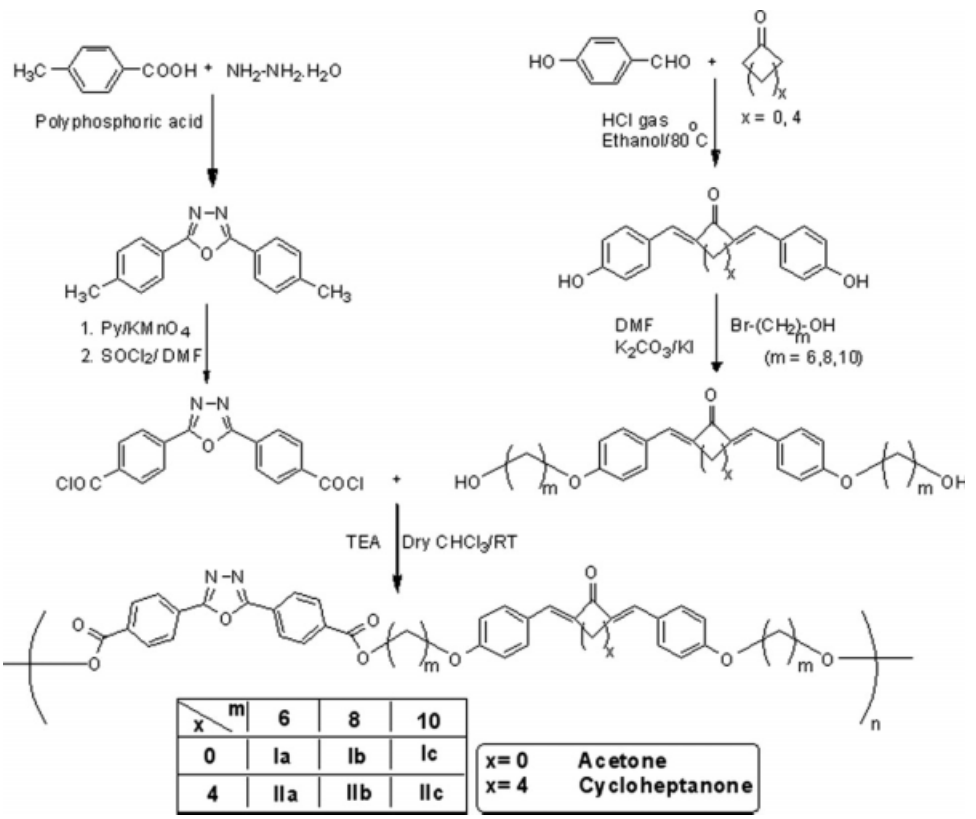

x \ m	6	8	10
0	Ia	Ib	Ic
4	IIa	IIb	IIc

Scheme 1 Synthesis of polymers **Ia–c and IIa–c**.

TABLE II
DSC and HOPM Data of Polymers Ia–Ic and IIa–IIc

Polymer	DSC (°C)				HOPM (°C)			
	T_g	T_m	T_i	ΔT	T_m	T_i	ΔT	Mesophase
Ia	62	146	175	29	149	177	28	Grainy
Ib	59	131	168	37	129	167	38	Nematic
Ic	58	125	165	40	127	166	39	Nematic
IIa	104	170	206	36	171	208	37	Grainy
IIb	98	165	204	39	166	203	37	Nematic
IIc	74	158	203	45	159	204	45	Nematic

polycondensation method in the presence of triethylamine as HCl acceptor. Monomers and polymers were characterized spectroscopically.

The polymers were soluble in chloroform, dichloromethane, dimethylformamide, and THF due to flexible methylene chains and polarity of ester linkage but insoluble in methanol, ethanol, 2-propanol, benzene, and toluene. Intrinsic viscosity was determined by Ubbelohde viscometer in chloroform solution at 30°C are in the range of 0.54–1.02 dl g^{-1} and revealed that the viscosity increased with increasing length of aliphatic chains (Table I). Elemental analysis of **Ia–c** and **IIa–c** revealed that the found values are in accordance with the calculated values. The data are listed in Table I.

Mesomorphic property

DSC measurements and polarizing optical microscopic observations were performed to confirm the existence of mesomorphic behavior of polymers. Table II displays the variation in transition temperatures with "*m*". Figure S1 (Supporting Information) represents DSC curves of **Ia–c** and **IIa–c** and indicates three well-separated endothermic transitions correspond to glass transition temperature (T_g), crystalline-liquid crystalline (T_m), and liquid crystalline-isotropic transitions (T_i), respectively.

DSC analysis indicated the T_m and T_i of **Ia–c** and **IIa–c**, they were decreased with an increase in flexible methylene chain and *vice versa*.[33] Correlation between methylene spacers, T_m, and T_i obtained from DSC are shown in Figure 1 and suggest a linear relationship with T_m and T_i of polymers which decreased with increasing spacer lengths. T_m of **Ia–c** and **IIa–c** are in the range of 125–146°C and 158–170°C, respectively. DSC data disclosed that T_g values increases with decreasing spacer lengths.[34]

Figure 2 depicts representative microphotograph of **Ib**, **Ic**, and **IIc** during first cooling cycle at 20× magnification, suggested enantiotropic LC phase and type of mesophase textures and are given in Table II. It was inferred that ΔT of **Ia–c** and **IIa–c** are in the range of 28–39°C and 37–45°C, respectively. Polymer with lower methylene chains exhibited grainy texture, whereas higher methylene chains exhibited thread-like and schlieren textures of nematic mesophases ascribed to flexible methylene spacers separated the mesogenic alignment. Formation of nematic mesophase was further confirmed by observation of flashlight when applied with small mechanical stress on liquid crystalline melt.[35]

Apart from methylene spacers, 1,3,4-oxadiazole can also play an important role in pretending liquid crystallinity, which suppresses mesomorphic behavior assigned to nonlinearity or boomerang shape of mesogenic structure. It is ascribed to bend angle (134°) associated with exocyclic bond in 2 and 5-positions of oxadiazole unit is too severe to achieve requisite ordered packing in mesophases. If such structures could exhibit mesomorphism, severe bend in mesogenic core might restrict free rotation of mesogenic unit around its long dimension.

It was expected that there is a possibility of these polymers to exhibit biaxial nematic (N_b) texture due to 1,3,4-oxadiazole mesogen contains bent or boomerang shaped[36,37] with large exocyclic bond angle to display N_b texture. Furthermore, observation of two-brush disclinations due to elastic constant of biaxial nematic[38] was reported for substituted 1,3,4-oxadiazole-based polymers by Sing and Lin[39] and also in our previous report.[22] Nevertheless, such N_b texture was unnoticed through HOPM in this study, attributed to unfavorable geometry of molecules to provide sufficient elastic constant to produce biaxial nematic textures.

Thermal property

Thermal behavior of polymers was evaluated by TGA in nitrogen atmosphere at a heating rate of

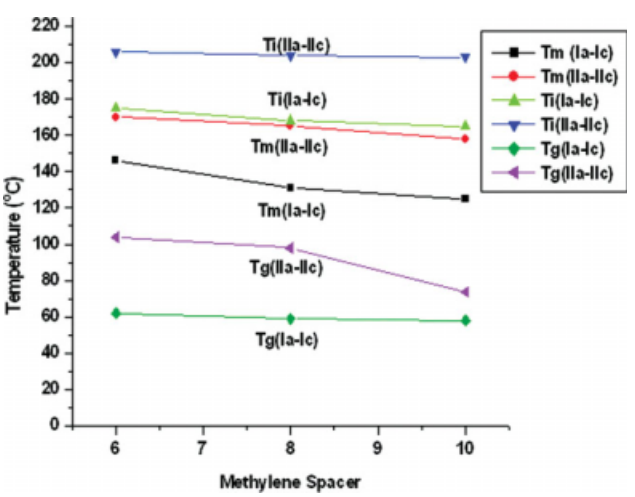

Figure 1 Correlation between T_m and T_i (DSC) with methylene spacer. [Color figure can be viewed in the online issue, which is available at www.interscience.wiley.com.]

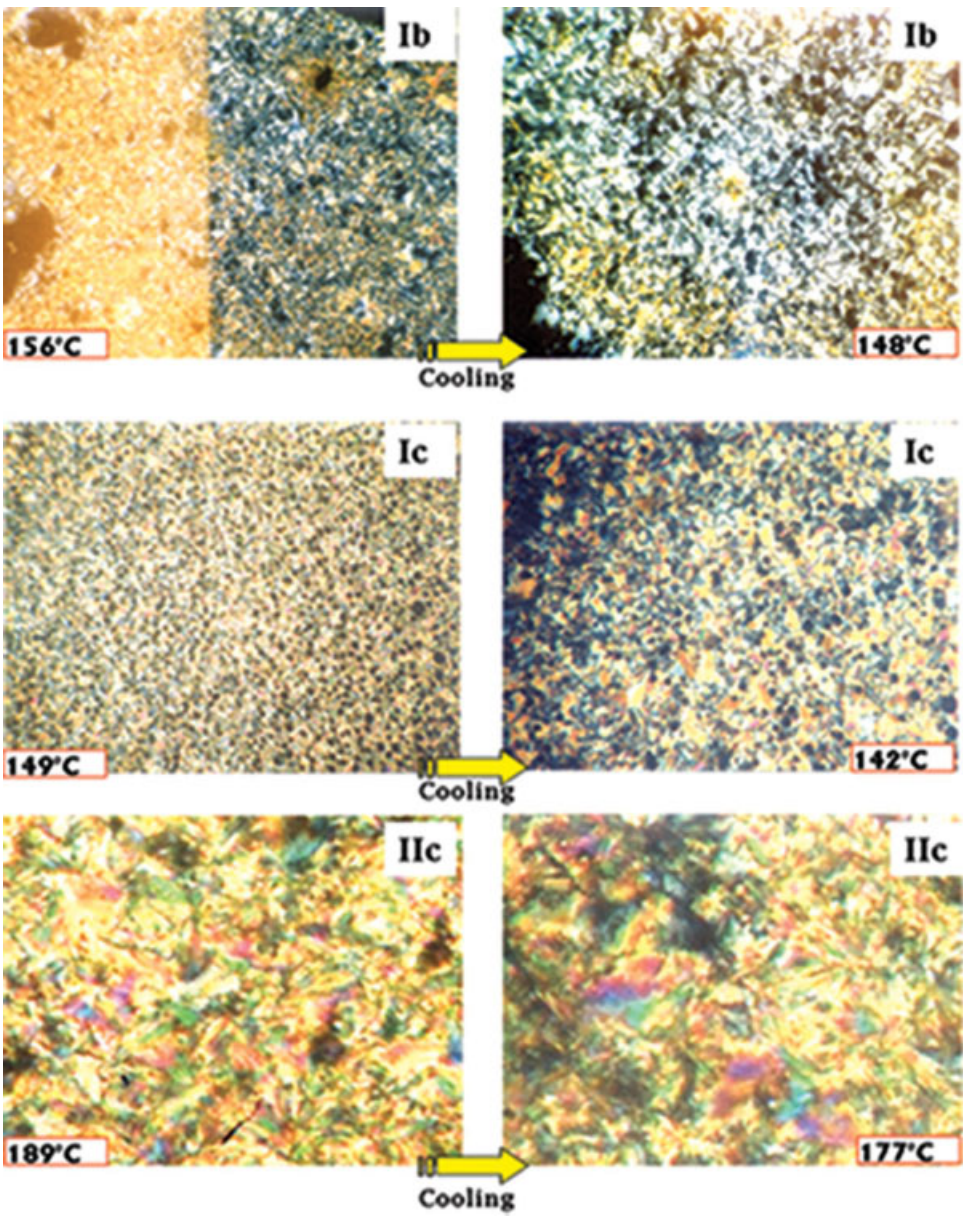

Figure 2 Representative HOPM photographs of **Ib**, **Ic**, and **IIc** at 20× magnifications. [Color figure can be viewed in the online issue, which is available at www.interscience.wiley.com.]

10°C/min, traces of polymers illustrated in Figures S2 and S3 (Supporting Information) and data given in Table III. Thermal stability of polymers was evaluated by 5% and 50% weight loss at minimum temperature. Results revealed that they were stable up to 310°C and start degrading thereafter in nitrogen. Thermal stability increases with decreasing spacer lengths [**Ia**>**Ib**>**Ic; IIa**>**IIb**>**IIc**] attributed to presence of ether linkage in the spacer units expected to introduce flexibility to polymer methylene chains and consequently brought down thermal stability.[40] It is noteworthy to mention that polymers containing cycloheptanone (350–375°C) were more stable than acetone (310–368°C) (**II** series > **I** series). Theoretical explanation based on Baeyer's strain theory revealed reverse trend ascribed to heat of combustion per methylene unit of acetone (assumed to be cyclopropanone) is higher than cycloheptanone,[41] because of more flexibility of acetone molecule reduces overall rigidity, and brought down thermal stability when compared with cycloheptanone containing polymers.

Degradation occurs in two-step manner; first step around 400°C corresponds to cleavage of ester linkage in the polymer[42] and second step between 575 and 625°C may be the outcome of cleavage in aryl–alkyl–ether linkages. Char yield were measured at 800°C and inferred that it increases with decreasing spacer lengths (**Ia** >**Ib**>**Ic and IIa** >**IIb** > **IIc**). Maximum char yield was noted for **Ia** (~31%) and minimum for **IIc** (~13%).

TABLE III
Thermal Decomposition Values of Polymers Ia–Ic and IIa–IIc

Polymer	TGA		
	5 % weight loss	50 % weight loss	carbine residue (%) at 800°C
Ia	368	460	31
Ib	325	445	27
Ic	310	440	21
IIa	375	468	28
IIb	362	463	20
IIc	350	495	13

Optical property

Optical property was studied both in chloroform solution and in thin film under UV irradiation and structural changes monitored by UV spectrophotometer. Figures 3 and 4 show change of UV–Vis spectra of polymer **Ic** both in solution (chloroform) and in thin film as a typical example for photochemical behavior upon irradiation at $\lambda > 300$ nm. As shown in Figure 6, during irradiation, a continuous decrease in absorption at 366 nm, due to π–π* transition of bisbenzylidene chromophores and increase of absorption band at 305 nm were noted with an isobestic point at 325 nm. Similar trend was noticed for remaining polymers.

Photoreaction of bisbenzylidene chromophore suggest that single and double bonds between two phenyl rings in bisbenzylidene chromophore are extensively conjugated with extended π-orbital between two phenyl rings and electron donor and acceptor characteristics of ether oxygen and carbonyl group, respectively.[43] Charge transfer interaction in bisbenzylidene chromophore as shown in Figure 5 reduces double bond characters between two phenyl rings and also increase bond order in the single

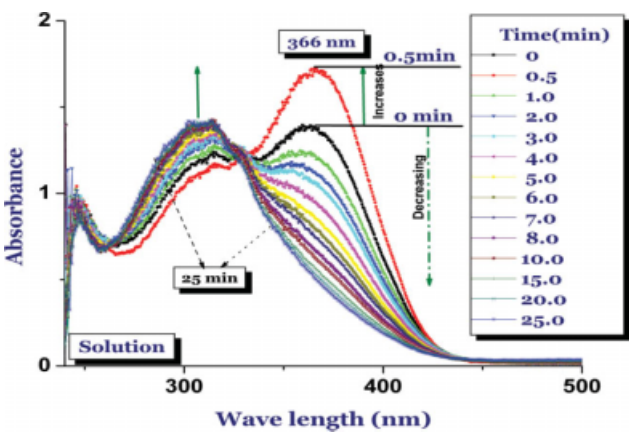

Figure 3 Changes in UV spectral characteristics during photolysis of **Ic** in chloroform solution at various time intervals. [Color figure can be viewed in the online issue, which is available at www.interscience.wiley.com.]

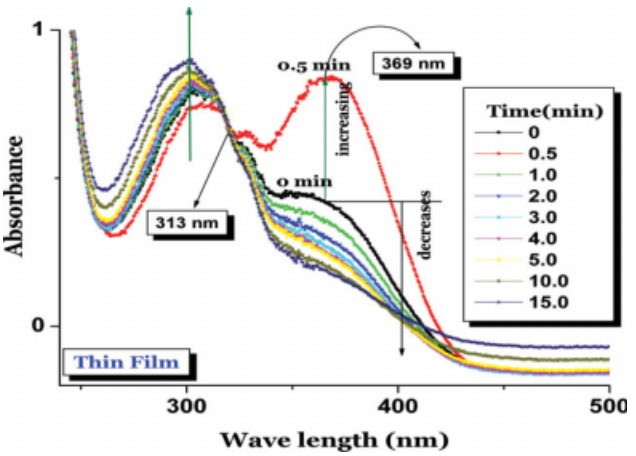

Figure 4 Changes in UV spectral characteristics during photolysis of **Ic** in thin film at various time intervals. [Color figure can be viewed in the online issue, which is available at www.interscience.wiley.com.]

bond, increases rotational barrier between *E*-Z and *E*-*E* chromophore.[22] The similar trend was detected for polymer **Ic** in thin film. As the exposure time was increased, concentration of *E*-isomer decreases, (*E*–π–π*, transition lowers, λ_{max} 369 nm), conversely, concentration of Z-isomer increases (Z–π–π* λ_{max} 303 nm) and a clear isobestic point noticed at 313 nm.

It is interesting to note that there is an increase in intensity as well as a small blue shift noticed at 366 nm for poly[bis(benzylidene)]acetone/cycloheptanone polyesters, during the first 0.5 min of irradiation. This increase in intensity reverses on further irradiation and decreases regularly thereafter. This increase has been assigned to disorganization caused by randomly oriented bisbenzy1ideneacetone/cycloheptanone chromophores as polymer changes to

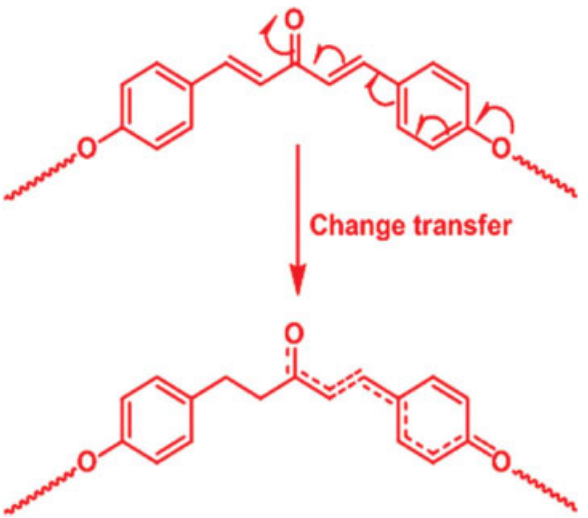

Figure 5 Charge transfer interaction in bisbenzylidene unit. [Color figure can be viewed in the online issue, which is available at www.interscience.wiley.com.]

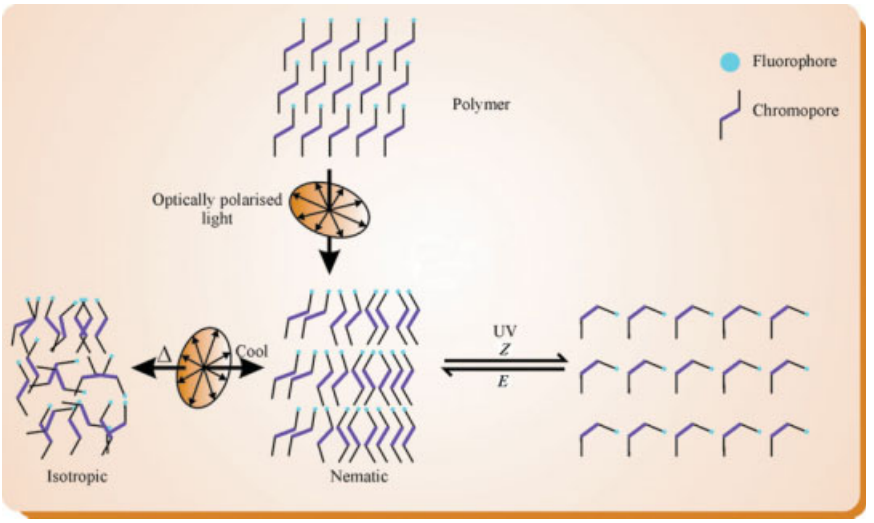

Figure 6 Phase diagram of photochemical phase transition of bisbenzylidene based polymers. [Color figure can be viewed in the online issue, which is available at www.interscience.wiley.com.]

isotropic state. This disordered structure could also be introduced by *E-to-Z* photoisomerization of bisbenzylidenecyclohexanone chromophores on irradiation. This kind of isomerization was well known in similar low-molecular-weight compounds[44] and disrupts parallel stacking of chromophores in aggregate attributed to nonlinear conformation of *Z*-isomer (Fig. 6). Similar results were noticed and reported by Gangadhara and Kishore.[45]

A possible [2+2] bisbenzylidene photo-dimerization product would be expected to exhibit tailing absorption near 250 nm and disappearance of olefinic protons in ^{1}H-NMR spectrum.[46] Such characteristics not observed for photoproduct derived from polymer **Ic** in solution, indicating photoisomerization process taken place in dilute solution.

To support this photoisomerization phenomenon, polymer samples were subjected to irradiation by UV light for a long time and then analyzed by solubility test, FTIR, DSC, and HOPM. The photo-irradiated polymers were found to be soluble in organic solvents and confirmed the photoisomerization process. In FTIR spectroscopy, the peak at 1710 cm^{-1} assigned to C=O carbonyl group conjugated with peak at 1635 cm^{-1} assigned to C=C double bond of chalcone moiety was not decreased and not shifted to higher wave number (Fig. 7) dotted line), which indicates that conjugated system of chalcone unbroken and no new bond formed after irradiation.

The liquid crystalline texture was unaltered in the irradiated sample of polymer **Ic** for a long time (4 h), and exhibited as observed before irradiation, testify photoisomerization process. There is an identical mesophase region between T_m and T_i was noticed for both before and after irradiated samples in DSC analysis (Fig. 8). Nevertheless, there is a slight difference in sharpness in endotherms noted in UV-treated sample when compared with that of nonirradiated sample, which is slightly broad. This difference in sharpness may be ascribed that during photoreaction, polymeric molecules absorb energy and organized themselves in a particular order to bring down charge transfer interaction in benzylidene chromophore. This charge transfer interaction reduces double bond character and increase single bond order thereby increases rotational barrier between *E-Z* chromophore. This charge transfer interaction may be the rationale for providing sharpness in irradiated when compared with nonirradiated sample.

In addition, a small hump was observed in UV-irradiated sample **Ib** and unnoticed the same in nonirradiated scan. This may be ascribed to

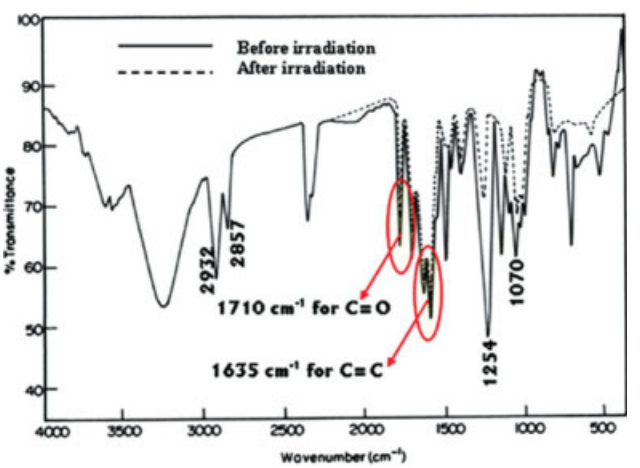

Figure 7 FTIR spectra of **Ib** before and after irradiation. [Color figure can be viewed in the online issue, which is available at www.interscience.wiley.com.]

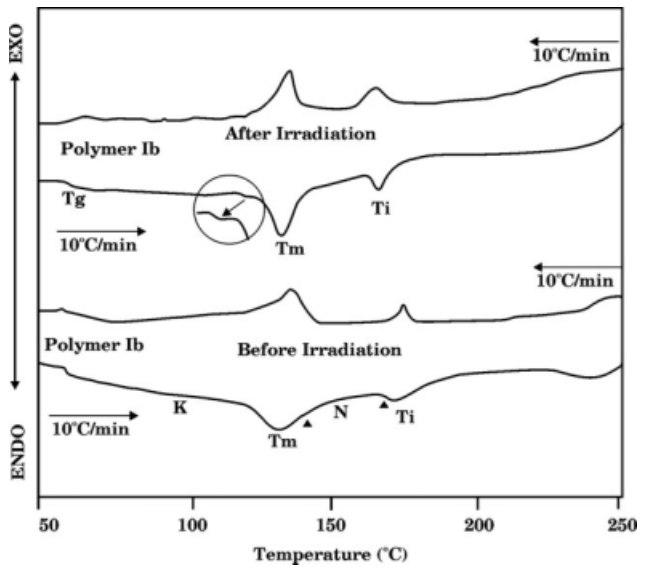

Figure 8 Before and after photo-irradiated **Ib** at heating and cooling cycles of DSC scans.

disruption of parallel stacking of chromophores in aggregate of nonlinear conformation of *Z*-isomer during irradiation.

Generally, photochemical phase transitions depend significantly on molecular shape of each isomer in photochromic molecules. Photochemical phase transitions are monitored most conveniently by setting LC sample between a pair of crossed polarizer and measuring transmittance of probe light through them. If the sample is in LC phase, nonzero transmittance observed due to birefringence, on the other hand, in isotropic phase, transmittance should be zero. Polarizing microscopic observation of irradiated LC sample acts in this manner. In *E*-form containing nematic LC sample dark spot was not observed in HOPM during the initial stage of photo irradiation. It suggests that the isotropic domains are not formed at the irradiated sites where sufficient amount of *Z*-form produced upon photo irradiation and nematic-isotropic phase transition not taken place in local domain (Fig. 6). This may be ascribed to *E* and *Z* isomer show a rod-like molecular structure, and *E*-Z isomerization produces little change in molecular shape. As a result, no photochemical mesophase transition was ascertained in LCPs during photo irradiation[47] as shown in Figure 8.

If photochromic moiety is a LC-azo derivative, it will show rigid rod shape in *E*-form, whereas *Z*-isomers show a bent shape. This difference in molecular shape will give rise to significant change in stabilization of mesophase structure of LCs. It intends that in an initial stage of photo irradiation of *E*-azobenzene containing nematic LC samples, dark spots were observed with polarizing microscope due to formation of isotropic domains at the irradiated sites; when sufficient amount of *Z*-azobenzenes produced on successive irradiation, the isotropic domains grow and area of dark spots increases and finally whole area becomes isotropic.[48] On the other hand, in this study, such changes were unnoticed in successive irradiation with bisbenzylidene chromophore.

Considering the photolysis of bisbenzylidene series, bisbenzylidene cyclohexanone and pentanone-based polymers showed photocrosslinking behavior, whereas bisbenzylidene acetone and cycloheptanone-based polymers exhibited photoisomerization, contrary to anticipated photocrosslinking behavior. This is attributed to unfavorable geometry of polymer molecule to provide sufficient conformational freedom to allow mesogenic units to form crosslinking during prolonged irradiation.

In addition to photolysis, the band gap energies (E_g) were calculated from absorption spectra for all the polymers according to the following equation:

$$E_g = hc/\lambda$$

Where h = Planck's constant (Js), c = velocity of light (m/s), and λ = wavelength (nm).

By using the earlier equation, band gap energies were calculated and found in the range of 3.18–3.41 eV.

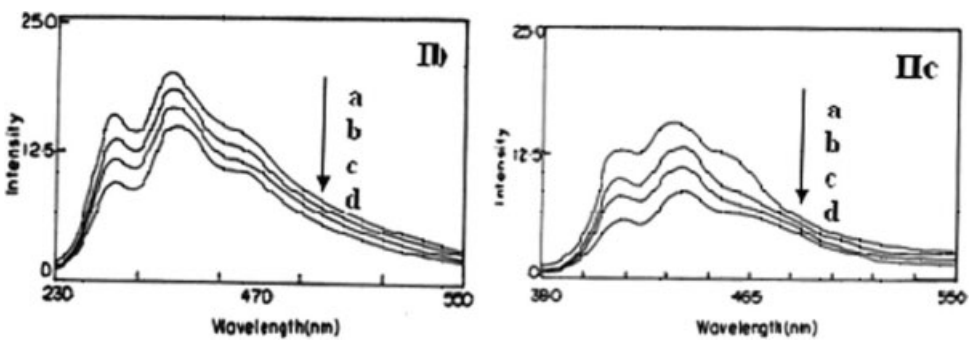

Figure 9 Representative emission traces of **Ib** and **IIc** in $CHCl_3$ solution at various concentrations (1×10^{-5}, 2×10^{-5}, 5×10^{-5}, and 15×10^{-5}).

TABLE IV
Optical Data of Polymers Ia–Ic and IIa–IIc Measured in $CHCl_3$ Solution

	Absorption spectra		Emission spectra	
Polymer	λ_{max} (nm)	E_g (eV)	λ_{max} (nm)	
Ia	389	3.18	409	438
Ib	364	3.40	410	437
Ic	366	3.38	410	436
IIa	363	3.41	411	437
IIb	364	3.40	412	437
IIc	363	3.41	412	438

Photoluminescence study

The emission spectra of polymers in chloroform solution at various concentrations were investigated; representative emission traces of polymer **Ib** and **IIc** were shown in Figure 9 and data listed in Table IV. Blue-emission maxima observed in PL spectra in solution between 409 and 438 nm, when excited at 363–389 nm, which were red shifted by 46–49 nm. This shift ascribed to electronic effect lowers the LUMO level and reduces the energy gap.[49] As shown in Figure 9, all the spectra shows two maxima peaks at 409 and 438 nm, this represents blue emission and their edges are beyond 500 nm. It was found that as the solution concentration increased, the relative ratio of two peaks at about 409 and 438 nm changed; suggesting the energy transfer occurred in concentrated solution, resulting in more intensive peak at 438 nm. Moreover, it was noted that all the polymers showed almost similar emission maxima in the emission spectra attributed to emission is insensitive irrespective of spacer length in the polymers.[50]

CONCLUSIONS

Photoisomerization behavior in chalcone unit was investigated in nematic main chain polyesters and strongly evidenced by solubility, carbonyl bands in FTIR, existence of mesophases by HOPM, and DSC analysis of prolonged irradiated polymer samples. HOPM results showed that all polymers exhibited enantiotropic nematic liquid crystalline property and formation of grainy and nematic threads depend on spacer lengths, enantiotropic LCPs exhibited remarkable spacer effect on increasing mesophase transitions (ΔT) with increasing spacer lengths, which were further supported by DSC analysis. Structure–property relationships were probed by correlating the spacer length with development of mesophase formation, thermal, and optical properties. Optical property of polymers brought out photoisomerization phenomena. Band gap energies were found to be in the range of 3.18–3.41 eV. Fluorescence spectra in solution indicated that emission maxima were elicited at 409 and 438 nm with Stoke shifts being 46–49 nm. These results show the prominence of flexible spacer in understanding the mesophase structure and property for the polyesters. The *Z–E* behavior of these polymers may be suitably exploited for optical switching applications as like azobenzene polymers.

The author R.B. gratefully acknowledges the Council of Scientific and Industrial Research (CSIR) New Delhi, India, for the award of Senior Research Fellowship.

References

1. Penny, S.; Barny, P. L. Liq Cryst 2000, 27, 329.
2. Ichimura, K. Supramol Sci 1996, 3, 67.
3. Rehab, A.; Salahuddin, N. Polymer 1999, 40, 2197.
4. Ichimura, K. Chem Rev 2000, 100, 1847.
5. Tomita, H.; Kudo, K.; Ichimura, K. Liq Cryst 1996, 20, 171.
6. Isayev, A. I.; Kyu, T.; Cheng, S. Z. D., Eds. Liquid Crystalline Polymer Systems: Technological Advances. ACS Symposium Series No 632; ACS: Washington, DC, 1996.
7. Lakowicz, J. R. Principles of Fluorescence Spectroscopy; Plenum Press: New York, 1986.
8. Winnik, M. A., Ed. Photophysical and Photochemical Tools in Polymer Science (Conformation, Dynamics, Morphology). NATO ASI series; Reidel: Dordrecht, 1986.
9. Itagaki, H.; Horie, K.; Mita, I. Prog Polym Sci 1990, 15, 361.
10. Huang, H. W.; Horie, K.; Masatoshi, T.; Watanabe, J. Macromol Chem Phys 1998, 199, 1851.
11. Strukelj, M.; Papadimitrakopoulos, F.; Miller, T. M.; Rothberg, L. J. Science 1995, 267, 1969.
12. Ahn, J. H.; Wang, C.; Pearson, C.; Bryce, M. R.; Petty, M. C. Appl Phys Lett 2004, 85, 1283.
13. Bao, Z..; Peng, Z.; Galvin, M. E.; Chandross, E. A. Chem Mater 1998, 10, 1201.
14. Chen, Z.. K.; Meng, H.; Lai, Y. H.; Huang, W. Macromolecules 1999, 32, 4351.
15. Pei, Q.; Yang, Y. Chem Mater 1995, 7, 1568.
16. Peng, Z.; Bao, Z.; Galvin, M. E. Chem Mater 1998, 10, 2086.
17. Kulkarni, A. P.; Tonzola, C. J.; Babel, A.; Jenekhe, S. A. Chem Mater 2004, 16, 4556.
18. Hughes, G.; Bryce, M. R. J Mater Chem 2005, 15, 94.
19. Mikroyannidis, J. A.; Spiliopoulos, I. K.; Kasimis, T. S.; Kulkarni, A. P.; Jenekhe, S. A. Macromolecules 2003, 36, 9295.
20. Huang, W.; Meng, H.; Yu, W. L.; Pei, J.; Chen, Z.. K.; Lai, Y. H. Macromolecules 1999, 32, 118.
21. Balamurugan, R.; Kannan, P. J Polym Sci Part A: Polym Chem 2008, 46, 5760.
22. Shin, D. M.; Song, D. M.; Jung, K. H.; Moon, J. H. J Photosci 2001, 8, 9.
23. Furniss, B. S.; Hannaford, J.; Smith, P. W.; Tatchile, A. R. Vogel's Textbook of Practical Organic Chemistry, 5th ed.; ELBS: London, 1994.
24. Perrin, D. D.; Armarego, W. L. F. Purification of Laboratory Chemicals, 3rd ed.; Pergamon press: New York, 1988.
25. Camps, F.; Gasol, V.; Guerrero, A. Synthesis 1987, 5, 511.
26. Bringmann, G.; Schneider, S. Synthesis 1983, 2, 139.
27. Kang, S. K.; Kim, W. S.; Moon, B. H. Synthesis 1985, 12, 1161.
28. Borden, D. S. J Appl Polym Sci 1978, 22, 239.
29. Seigrist, A. E.; Dunnenberger, E. M. Swiss Pat. 383,985 (1965); Chem Abstr 1965, 62, 14867c.
30. Percec, V.; Marian, N. H.; Sami, N.; Morrison, J. J.; Glodde, M.; Jan, S.; Peterca, M.; Brad Rosen, M.; Uchida, S.;

Balagurusamy, V. S. K.; Monica, J. S.; Paul, A. H. Chem Eur J 2006, 12, 6216.
31. Tomlinson, R. V.; Tener, G. M. J Org Chem 1964, 29, 493.
32. Sakthivel, P.; Kannan, P. J Polym Sci Part A: Polym Chem 2004, 20, 5215.
33. Senthil, S.; Kannan, P. J Polym Sci Part A: Polym Chem 2001, 39, 2396.
34. Kannan, P.; Senthil, S.; Vijayakumar, R.; Marimuthu, R. J Appl Polym Sci 2002, 86, 3494.
35. Wu, S. L.; Chen, F. D. Liq Cryst 2003, 30, 991.
36. Kishikawa, K.; Harris, M. C.; Swager, T. M. Chem Mater 1999, 11, 867.
37. Dingemans, T. J.; Samulski, E. T. Liq Cryst 2000, 27, 131.
38. Chandrasekhar, S.; Nair, G. G.; Rao, D. S. S.; Praefcke, K.; Blunk, D. Liq Cryst 1998, 24, 67.
39. Sung, H. H.; Lin, H. C. Liq Cryst 2004, 31, 831.
40. Aly, K. I.; Khalaf, A. A.; Alkskas, I. A. Eur Polym J 2003, 39, 1035.
41. Morrison, R. D.; Boyd, R. N. Organic Chemistry; Prentice Hall India: New Delhi, 1953.
42. Guo, W.; Leu, W. T.; Hsiao, S. H.; Liou, G. S. Polym Degrad Stab 2006, 91, 21.
43. Oumi, M. D.; Maurice, D.; Gordon, M. H. Spectrochim Acta A Mol Biomol Spectrosc 1999, 55, 525.
44. Aizeshtat, Z..; Hausmann, M.; Pickholtz, Y.; Tal, D.; Blum, J. J Org Chem 1977, 42, 2386.
45. Gangadhara, K. Macromolecules 1995, 28, 806.
46. Wolf, M. O.; Fox, M. A. Langmuir 1996, 12, 955.
47. Sung, J. H.; Hirano, S.; Tsutsumi, O.; Kanazawa, A.; Shiono, T.; Ikeda, T. Chem Mater 2002, 14, 385.
48. Ikeda, T. J Mater Chem 2003, 13, 2037.
49. Wong, M. S.; Li, Z.. H.; Tao, Y.; D'ioro, M. Chem Mater 2003, 15, 1198.
50. Hsu, W. H.; Kazuyuki, H.; Masatoshi, T.; Watanabe, J. Polymer 1999, 40, 3013.